

RESEARCH ARTICLE

ω 3 fatty acid metabolite, 12-hydroxyeicosapentaenoic acid, alleviates contact hypersensitivity by downregulation of *CXCL1* and *CXCL2* gene expression in keratinocytes via retinoid X receptor α

Azusa Saika^{1,2} | Takahiro Nagatake¹ | So-ichiro Hirata¹ | Kento Sawane^{1,2,3} | Jun Adachi⁴ | Yuichi Abe^{4,5} | Junko Isoyama⁴ | Sakiko Morimoto¹ | Eri Node¹ | Prabha Tiwari¹ | Koji Hosomi¹ | Ayu Matsunaga^{1,6} | Tetsuya Honda^{7,8} | Takeshi Tomonaga⁴ | Makoto Arita^{9,10,11} | Kenji Kabashima⁷ | Jun Kunisawa^{1,2,12,13,14}

¹Laboratory of Vaccine Materials, Center for Vaccine and Adjuvant Research and Laboratory of Gut Environmental System, National Institutes of Biomedical Innovation, Health and Nutrition (NIBIOHN), Osaka, Japan

²Graduate School of Pharmaceutical Sciences, Osaka University, Osaka, Japan

³Nippon Flour Mills Co., Ltd, Innovation Center, Atsugi, Japan

⁴Laboratory of Proteome Research and Laboratory of Proteomics for Drug Discovery, NIBIOHN, Osaka, Japan

⁵Division of Molecular Diagnosis, Aichi Cancer Center Research Institute, Nagoya, Japan

⁶Department of Food and Life Science, School of Life and Environmental Science, Azabu University, Sagamihara, Japan

⁷Department of Dermatology, Kyoto University Graduate School of Medicine, Kyoto, Japan

⁸Department of Dermatology, Hamamatsu University School of Medicine, Shizuoka, Japan

⁹Division of Physiological Chemistry and Metabolism, Faculty of Pharmacy, Keio University, Tokyo, Japan

¹⁰Laboratory for Metabolomics, RIKEN Center for Integrative Medical Sciences, Yokohama, Japan

¹¹Cellular and Molecular Epigenetics Laboratory, Graduate School of Medical Life Science, Yokohama City University, Yokohama, Japan

¹²Department of Microbiology and Immunology, Kobe University Graduate School of Medicine, Kobe, Japan

¹³International Research and Development Center for Mucosal Vaccines, The Institute of Medical Science, The University of Tokyo, Tokyo, Japan

¹⁴Graduate School of Medicine, Graduate School of Dentistry, Osaka University, Suita, Japan

Correspondence

Jun Kunisawa, Laboratory of Vaccine Materials, Center for Vaccine and Adjuvant Research and Laboratory of Gut Environmental System, National Institutes of Biomedical Innovation, Health and Nutrition (NIBIOHN), 7-6-8 Saito-Asagi, Ibaraki, Osaka 567-0085, Japan.

Abstract

ω 3 fatty acids show potent bioactivities via conversion into lipid mediators; therefore, metabolism of dietary lipids is a critical determinant in the properties of ω 3 fatty acids in the control of allergic inflammatory diseases. However, metabolic progression of ω 3 fatty acids in the skin and their roles in the regulation of skin inflammation

Abbreviations: CHS, contact hypersensitivity; CXCL, C-X-C motif chemokine ligand; CYP, cytochrome P450; diHETE, dihydroxyeicosatetraenoic acid; DAPI, 4',6-diamidino-2-phenylindole; DMEM, Dulbecco's modified Eagle's medium; DNFB, 2,4-dinitrofluorobenzene; EPA, eicosapentaenoic acid; EpETE, epoxyeicosatetraenoic acid; FITC, fluorescein isothiocyanate; fMLP, *N*-formylmethionyl-leucyl-phenylalanine; HEPE, hydroxyeicosapentaenoic acid; IFN- γ , interferon- γ ; iSALT, inducible skin-associated lymphoid tissue; i.p., intraperitoneal; LC-MS/MS, liquid chromatography-tandem mass spectrometry; LOX, lipoxygenase; LXR, liver X receptor; NF- κ B, nuclear factor- κ B; PPAR, peroxisome proliferator-activated receptor; RvE, resolvin E; RXR, retinoid X receptor; TNF- α , tumor necrosis factor- α .

This is an open access article under the terms of the Creative Commons Attribution-NonCommercial License, which permits use, distribution and reproduction in any medium, provided the original work is properly cited and is not used for commercial purposes.

© 2021 The Authors. *The FASEB Journal* published by Wiley Periodicals LLC on behalf of Federation of American Societies for Experimental Biology.

Email: kunisawa@nibiohn.go.jp

Funding information

Ministry of Education, Culture, Sports, Science and Technology of Japan (MEXT); Japan Society for the Promotion of Science KAKENHI, Grant/Award Number: JP19K07617, 19K08790, 15H05897, 18H02674, 18H02150, 15H05790 and 20H00534; Japan Agency for Medical Research and Development (AMED, Grant/Award Number: JP20ek0410062s0202, JP19gm1210006, JP20ek0410062h0002, JP20ak0101068h0004 and JP20gm1010006h004; Ministry of Health and Welfare of Japan; Public/Private R&D Investment Strategic Expansion Program: PRISM; Cross-ministerial Strategic Innovation Promotion Program: SIP; Grant for Joint Research Project of the Institute of Medical Science; University of Tokyo; Ono Medical Research Foundation; Canon Foundation

remains to be clarified. In this study, we found that 12-hydroxyeicosapentaenoic acid (12-HEPE), which is a 12-lipoxygenase metabolite of eicosapentaenoic acid, was the prominent metabolite accumulated in the skin of mice fed ω 3 fatty acid-rich linseed oil. Consistently, the gene expression levels of *Alox12* and *Alox12b*, which encode proteins involved in the generation of 12-HEPE, were much higher in the skin than in the other tissues (eg, gut). We also found that the topical application of 12-HEPE inhibited the inflammation associated with contact hypersensitivity by inhibiting neutrophil infiltration into the skin. In human keratinocytes in vitro, 12-HEPE inhibited the expression of two genes encoding neutrophil chemoattractants, *CXCL1* and *CXCL2*, via retinoid X receptor α . Together, the present results demonstrate that the metabolic progression of dietary ω 3 fatty acids differs in different organs, and identify 12-HEPE as the dominant ω 3 fatty acid metabolite in the skin.

KEYWORDS

12-hydroxyeicosapentaenoic acid, allergic contact dermatitis, keratinocytes, lipid metabolite, retinoid X receptor

1 | INTRODUCTION

Allergic contact dermatitis is a common skin disease characterized by inflammatory reactions such as edema and erythema at sites on the body that have come into contact with a type of allergen known as a hapten, which are low-molecular weight molecules with the ability to cross the skin barrier.^{1,2} Contact hypersensitivity (CHS) is a widely used animal model of human allergic contact dermatitis, and the development of CHS consists of two phases—sensitization phase and elicitation phase. In the sensitization phase, exposure to a hapten activates keratinocytes to produce various pro-inflammatory mediators that promote the migration of skin dendritic cells to the draining lymph nodes where they activate naïve T cells.^{3,4} In the elicitation phase, re-exposure of the skin to the same hapten again stimulates keratinocytes to release pro-inflammatory mediators, such as tumor necrosis factor- α (TNF- α), which induce the keratinocytes to produce the neutrophil chemoattractants C-X-C motif chemokine ligand (CXCL) 1 and CXCL2.⁴⁻⁷ Blockade of CXCL1 by neutralizing antibody or deficiency of CXCL1 and CXCL2 receptor, CXCR2, prevents CHS,⁸⁻¹⁰ suggesting that signaling by these chemokines is essential for the development of CHS. Also, exposure of the skin to the hapten activates tissue-resident mast cells, which enhance vascular permeability via the production of pro-inflammatory mediators such as histamine and TNF- α .¹¹ Together, these inflammatory events induce and accelerate neutrophil infiltration into the skin.

Once in the skin, the infiltrated neutrophils release reactive oxygen species, granule-derived mediators (eg, leukotriene B₄, defensins, and elastase), and pro-inflammatory

cytokines that induce skin edema and injury.¹²⁻¹⁸ Depletion of neutrophils by administration of a cell-specific antibody has been shown to decrease ear swelling, indicating that neutrophils play major roles in the development of CHS.^{16,19,20} The activated keratinocytes also produce CXCL9 and CXCL10, which guide the migration of memory CD8⁺ T cells to the inflamed skin.⁵ The infiltrated memory CD8⁺ T cells are further activated by dendritic cells located in inducible skin-associated lymphoid tissues (iSALT), which are composed of clusters of skin dendritic cells and infiltrated T cells.²¹ iSALT development is induced via chemokines produced by M2 macrophages in the skin that have been activated by keratinocyte-derived cytokines such as interleukin-1 α .²² Infiltrated T cells activated by dendritic cells in iSALT produce pro-inflammatory cytokines, such as interferon- γ (IFN- γ), that are essential for the induction of CHS.^{21,23-25} These pro-inflammatory cytokines also stimulate the production of inflammatory chemokines by keratinocytes, which amplifies the inflammatory response.^{26,27}

ω 3 fatty acids such as α -linolenic acid, eicosapentaenoic acid (EPA), and docosahexaenoic acid show beneficial effects on the control of inflammatory and allergic diseases such as inflammatory bowel disease, asthma, allergic conjunctivitis, food allergy, and atopic dermatitis; however, the underlying mechanisms remain to be investigated.²⁸⁻³⁵ Recent studies using liquid chromatography-tandem mass spectrometry (LC-MS/MS) have indicated that dietary ω 3 fatty acids are metabolized by enzymes such as lipoxygenase (LOX) and cytochrome P450 (CYP), resulting in the generation of lipid metabolites that exhibit potent pro-resolution, anti-inflammatory, and anti-allergic activities.³⁶

We previously reported that a diet including α -linolenic acid-rich linseed oil led to the elevation of an EPA-derived CYP metabolite, 17,18-epoxyeicosatetraenoic acid (17,18-EpETE), in the murine intestine, and that 17,18-EpETE alleviated allergic diarrhea in a mouse model of food allergy.³³ We also identified 15-hydroxyeicosapentaenoic acid (15-HEPE) as an EPA-derived metabolite generated by 15-LOX that dampens allergic rhinitis in the murine nasal passage.³⁷ Together, these observations suggest that different tissues generate different ω 3 fatty acid metabolites, and that some of these metabolites have actions that reduce inflammatory and allergic symptoms. In the present study, we aimed to extend our knowledge by analyzing EPA-derived metabolites in the skin and identified 12-HEPE as an ω 3 fatty acid-derived metabolite for the control of allergic contact dermatitis.

2 | MATERIALS AND METHODS

2.1 | Animals

Wild-type C57BL/6 and BALB/c female mice (age, 6-7 weeks) were purchased from Japan SLC (Shizuoka, Japan) and CLEA Japan (Tokyo, Japan), and kept in a specific-pathogen-free animal facility at the National Institutes of Biomedical Innovation, Health and Nutrition (NIBIOHN, Osaka, Japan) for at least 1 week before use in experiments. For the analysis of fatty acid metabolites in the skin and gut, mice were maintained for 2 months on diets composed of chemically defined food containing 4% (wt/wt) soybean oil or linseed oil (Oriental Yeast Co., Ltd., Tokyo, Japan).³³ Mice were killed by cervical dislocation under anesthesia with isoflurane (Forane, AbbVie, North Chicago, IL, USA). All experiments were performed in accordance with the guidelines of the Animal Care and Use Committee and the Committee on the Ethics of Animal Experiments at NIBIOHN.

2.2 | Induction of CHS

CHS was induced as described previously.³⁸ Briefly, mice were treated on shaved abdominal skin with 25 μ L of 0.5% (vol/vol) 2,4-dinitrofluorobenzene (DNFB; Nacalai Tesque, Kyoto, Japan) in 4:1 acetone:olive oil (Nacalai Tesque). After 5 days, both sides of the ears were challenged with 10 μ L of 0.2% (vol/vol) DNFB. Two days later, ear thickness was measured with a micrometer (model MDC-25MJ 293-230, Mitsutoyo, Kanagawa, Japan). To evaluate fatty acid activity, mice were treated with 12(*S*)-HEPE (Cayman Chemical, Ann Arbor, MI, USA), 12(*R*)-HEPE (Cayman Chemical), (\pm)12-HEPE (12-HEPE; Cayman Chemical), (\pm)15-HEPE (15-HEPE; Cayman Chemical), or (\pm)18-HEPE (18-HEPE; Cayman Chemical) via intraperitoneal (i.p.) injection

(100 ng/administration) or topical application to the skin (1 μ g/administration), 30 minutes before both sensitization and elicitation by DNFB treatment. The vehicle controls for i.p. injection and topical application were 0.5% (vol/vol) and 50% (vol/vol) ethanol in PBS (Nacalai Tesque), respectively.

To evaluate 12-HEPE actions via retinoid X receptor (RXR), the skin of the abdomen or ear was treated with 40 nmol of the RXR pan-antagonist HX 531 (Cayman Chemical) 60 minutes before 12-HEPE treatment for both sensitization and elicitation. The vehicle control for the topical application was 25% (vol/vol) dimethyl sulfoxide in PBS.

2.3 | Dendritic cell migration assay

Fluorescein isothiocyanate (FITC)-induced cutaneous dendritic cell migration assay was performed as described previously.³⁹ Two hundred microliters of 1% (wt/vol) FITC (Sigma-Aldrich, Saint Louis, MO, USA) dissolved in a 1:1 (vol/vol) acetone and dibutyl phthalate mixture were topically applied to the shaved abdomen of mice. 12-HEPE (1 μ g/administration) or vehicle (50% [vol/vol] ethanol in PBS) was topically applied to the abdominal skin 30 minutes before the topical application of FITC, and the draining lymph nodes of the axillary lymph nodes were collected 24 hours after FITC application. The activity of 12-HEPE was also examined by topical application at 24 hours after the topical application of FITC, and then, the draining lymph nodes were collected 48 hours after FITC application. Flow cytometry was used to count the number of FITC-bearing dendritic cells in the draining lymph nodes to evaluate the migration of cutaneous dendritic cells.

2.4 | Cell isolation and flow cytometric analysis

The isolation of cells from ear tissue and their flow cytometric analysis were performed as described previously.³⁸ Briefly, ear skin was digested in RPMI 1640 medium (Sigma-Aldrich) containing 2 mg/mL of collagenase (Wako, Tokyo, Japan) for 90 minutes at 37°C with stirring, and cell suspensions were filtered using a cell strainer (pore size, 100 μ m; BD Biosciences, Franklin Lakes, NJ, USA). Axillary lymph nodes were digested in RPMI 1640 medium containing 0.5 mg/mL of collagenase for 15 minutes at 37°C with stirring, and cell suspensions were filtered using a cell strainer (pore size, 100 μ m). The digestion and filtration operations were conducted a total of two times.

For flow cytometric analysis, cell suspensions in 2% (vol/vol) newborn calf serum in PBS were stained with anti-CD16/32 antibody (TruStain FcX, BioLegend, San Diego, CA, USA; 1:100) to avoid nonspecific staining. After

washes, the cells were further stained with the following antibodies: FITC-anti-Ly6G (BioLegend, 127606), allophycocyanin-Cy7-anti-CD11b (BioLegend, 101226), FITC-anti-CD8 α (BioLegend, 100706), allophycocyanin-anti-TCR β (BioLegend, 109212), phycoerythrin-anti-CD31 (BD Biosciences, 553373), FITC-anti-CD34 (BD Biosciences, 553733), allophycocyanin-anti-CD49f (BioLegend, 313616), AF647-anti-I-A^b (BioLegend, 116412), and BV421-anti-CD45 (BioLegend, 103133). Dead cells were detected using 7-aminoactinomycin D (BioLegend, 420404; 1:100) and were excluded from the analysis. For detection of intracellular cytokines, cells were treated for 60 minutes with brefeldin A (BioLegend) during collagenase treatment. The resultant cells were fixed and permeabilized with a Cytofix/Cytoperm Fixation/Permeabilization Kit (BD Biosciences). Intracellular cytokines were stained with phycoerythrin-anti-IFN- γ (BioLegend, 505808; 1:100). Mouse keratinocytes were isolated as CD45⁻ CD31⁻ CD34⁻ CD49f⁺ cell fraction as previously reported.⁴⁰ Samples were analyzed using a MACSQuant (Miltenyi Biotec, Bergisch Gladbach, Germany) or FACS Aria (BD Biosciences), and cells were sorted with the FACS Aria. Data were analyzed using FlowJo 9.9 software (TreeStar, Ashland, OR, USA).

2.5 | Histologic analysis

Histologic analysis was performed as described previously.³⁸ Briefly, ear samples were embedded in Tissue-Tek OCT Compound (Sakura Finetek, Tokyo, Japan) and frozen in liquid nitrogen. Frozen tissue sections (6 μ m) were prepared using a cryostat (model CM3050 S, Leica Biosystems, Wetzlar, Germany) and used for hematoxylin and eosin staining and immunohistologic analysis. The following antibodies were used: purified anti-mouse I-A/I-E mAb (BioLegend, 107602), purified anti-mouse CD3e mAb (BioLegend, 100302), Alexa Fluor 488-anti-rat IgG (Thermo Fisher Scientific, Waltham, MA, A-11006), Cy3-anti-Armenian hamster IgG (Jackson ImmunoResearch Laboratories, West Grove, PA, USA, 127-165-160), and FITC-anti-Ly6G mAb. Cell nuclei were stained with 4',6-diamidino-2-phenylindole (DAPI; AAT Bioquest, Sunnyvale, CA, USA). The stained tissue sections were examined under a fluorescence microscope (model BZ-9000, Keyence, Osaka, Japan).

2.6 | Vascular permeability assay

The vascular permeability assay was performed as described previously with some modifications.⁴¹ Two days after elicitation with DNFB, mice were intravenously administered Evans blue dye (1% [wt/vol] in PBS). One hour after administration, the mice were sacrificed and their ears were

collected. The ears were incubated in 1 mL of 3 mol/L KOH (Nacalai Tesque) at 37°C overnight to extract the Evans blue dye. Afterward, 1 mL of 1.24 mol/L H₃PO₄ and 3 mL of acetone were added and the mixture was centrifuged at 1280 g at 20°C for 15 minutes. The resultant solution was left to phase-separate at room temperature for 30 minutes. The supernatant was collected and absorbance (OD₆₂₀) was determined with a SmartSpec Plus (Bio-Rad Laboratories, Hercules, CA, USA). The concentration of Evans blue dye was determined using a standard curve of known amounts of the dye.

2.7 | Lipid extraction and LC-MS/MS analysis of EPA-derived metabolites

Lipid extraction was performed as previously reported.⁴² Briefly, lipids were obtained using a Monospin C₁₈-AX centrifugal column with deuterium-labeled internal standard.

LC-MS/MS was performed as described previously with modifications.^{42,43} Lipid metabolites were analyzed either with an ultra-high-pressure LC system (AQUITY, Waters, Milford, MA, USA) coupled with a hybrid ion trap-orbitrap mass spectrometer (Orbitrap ELITE; Thermo Fisher Scientific) with an Acquity UPLC BEH C₁₈ column (Waters)⁴² or a linear ion-trap quadrupole (QTRAP 5500, AB Sciex, Foster city, CA, USA) with an Acquity UPLC BEH C₁₈ column,⁴³ or a Shimadzu LCMS-8050 system with a triple quadrupole mass spectrometer (Shimadzu, Kyoto, Japan) with a Kinetex C₈ column (Shimadzu). Data were analyzed using Xcalibur software (Thermo Fisher Scientific) or Shimadzu Lab solution LCMS software (Shimadzu).

Deuterated internal standards were measured to check recoveries of lipid metabolites. For quantification of lipid metabolites, calibration curves were drawn using the following lipid standards obtained from Cayman Chemical: 5-HEPE, 12-HEPE, 15-HEPE, 18-HEPE, 17,18-EpETE, and 17,18-dihydroxyeicosatetraenoic acid (17,18-diHETE).

2.8 | Measurement of the amount of 12-HEPE in the skin

Mice were treated with 12-HEPE via i.p. injection or topical administration to the ear skin (1 μ g/administration) at 30 minutes before sacrifice. The ears were then collected for the measurement of 12-HEPE by LC-MS/MS.

2.9 | HaCaT cell culture

HaCaT cells were obtained from CLS Cell Lines Service (Eppelheim, Germany)⁴⁴ and grown in Dulbecco's modified Eagle's medium (DMEM) with high glucose (Sigma-Aldrich)

supplemented with 10% of fetal bovine serum (Gibco, Grand Island, NY, USA) and containing 100 U/mL of penicillin and 100 µg/mL of streptomycin (Nacalai Tesque) at 37°C and 5% CO₂. HaCaT cells were seeded in 96-well plates at 3×10^4 cells/well, and cultured for 24 hours. Then, the medium was replaced with DMEM without fetal bovine serum and the cells were treated first with 300 nM of 12-HEPE for 30 minutes and then, with 100 ng/mL of recombinant human TNF-α (Pepro Tech EC Ltd., London, UK) for 90 minutes. The vehicle control was 0.2% (vol/vol) ethanol in DMEM. The peroxisome proliferator-activated receptor (PPAR)γ antagonist GW9662 (Abcam, Cambridge, UK) was added 60 minutes before treatment with 12-HEPE and recombinant human TNF-α. The vehicle control was 0.2% (vol/vol) dimethyl sulfoxide in DMEM.

2.10 | Reverse transcription and quantitative real-time PCR analysis

Reverse transcription and quantitative real-time PCR were performed as described previously.³⁸ Briefly, total RNA was isolated from HaCaT cells or sorted cells using Sepasol-RNA I Super G (Nacalai Tesque). RNA samples were incubated with DNase I (Invitrogen, Carlsbad, CA, USA) and reverse-transcribed into cDNA using a Super Script VIRO cDNA Synthesis Kit (Invitrogen). RNA extraction from ears and gut was performed using a Relia Prep RNA Tissue Miniprep System (Promega, Tokyo, Japan) and reverse-transcribed. Quantitative real-time PCR analysis was performed with a LightCycler 480 II (Roche, Basel, Switzerland) with FastStart Essential DNA Probes Master (Roche). Primer sequences are described in Table S1.

2.11 | Isolation of neutrophils from bone marrow

Bone marrow-derived neutrophils were obtained as described previously.³⁸ Briefly, mice were killed and their femurs and tibias were used to isolate neutrophils. The bone marrow was flushed with RPMI 1640 medium containing 2% (vol/vol) of newborn calf serum using a syringe, and neutrophils were purified using 62% Percoll (GE Healthcare, Madison, WI, USA).

2.12 | Detection of actin polymerization in neutrophils

Actin polymerization was assayed as described previously.³⁸ Briefly, purified neutrophils (4×10^5 cells) were allowed to adhere to fibronectin-coated coverslips (Neuvitro Corporation,

Vancouver, WA, USA) for 15 minutes in a 5% CO₂ incubator. Neutrophils were treated with 12-HEPE (1 µmol/L) or 0.3% (vol/vol) ethanol in PBS (vehicle control) for 15 minutes and then, stimulated with 1 µmol/L of *N*-formylmethionyl-leucyl-phenylalanine (fMLP; Sigma-Aldrich) for 2 minutes in the incubator. Neutrophils were stained with 100 nmol/L of Acti-stain 488-phalloidin (Cytoskeleton, Denver, CO, USA), and cell nuclei were stained with DAPI. Images were obtained under a Leica TCS SP8 confocal microscope (Leica Microsystems, Wetzlar, Germany).

2.13 | Transfection of HaCaT cells with siRNA

HaCaT cells were cultured for 24 hours and then, transfected with 33 nM RXRα-specific siRNA (Hs_RXRA_3 FlexiTube siRNA; Qiagen, Hilden, Germany) or 33 nM silencer negative control siRNA (AllStars Negative Control siRNA; Qiagen) using Lipofectamine 2000 Transfection Reagent (Thermo Fisher Scientific) prepared in Opti-MEM I Reduced Serum Medium (Gibco) following the manufacturers' protocols. At 48 hours after transfection, the cells were transferred to a new dish and the siRNA transfection was repeated.

2.14 | Western blot analysis

Cells were washed with ice-cold PBS and lysed in RIPA Lysis Buffer (Merck Millipore, Billerica, MA, USA) containing protease-inhibitor cocktail (Sigma-Aldrich; 1:100) on ice using a cell scraper. The cell solution was left on ice for 30 minutes and then, centrifuged at 13000 *g* at 4°C for 15 minutes. The supernatant was retained as the total protein fraction and the total protein concentration was determined using a Pierce BCA Protein Assay Kit (Thermo Fisher Scientific). Ten microgram of protein from lysate cells was loaded onto NuPAGE 4%-12% Bis-Tris Gels (Invitrogen), electrophoretically separated, and transferred to an Immobilon-P transfer membrane (Merck Millipore). Afterward, the membrane was blocked with 5% (wt/vol) skim milk in PBS-T (0.5% [vol/vol] Tween-20 in PBS) for 60 minutes, and then, reacted with primary antibody, which was either anti-rabbit RXRα mAb (Cell Signaling Technology, Beverly, MA, USA, 3085S; 1:1000) or anti-mouse β-actin mAb (BioLegend, 643802; 1:1000) in Can Get Signal solution-1 (TOYOBO, Osaka, Japan) for 60 minutes. After washes with PBS-T, the membrane was reacted in Can Get Signal Solution-2 with horseradish peroxidase-conjugated secondary antibody, which was either donkey anti-rabbit IgG antibody (BioLegend, 406401; 1:5000) or goat anti-mouse IgG antibody (SouthernBiotech, Birmingham, AL, USA, 1030-05; 1:5000). Western blot

bands were visualized using an enhanced chemiluminescence detection reagent, Chemi-Lumi One L (Nacalai Tesque), and were determined using an LAS-4000 mini-luminescent image analyzer (GE Healthcare).

2.15 | Statistics

Statistical significance was evaluated using one-way ANOVA followed by the Kruskal-Wallis test and Mann-Whitney U test in Prism 3.03 software (GraphPad Software, San Diego, CA, USA). A *P*-value of less than 0.05 was considered significant.

3 | RESULTS

3.1 | Identification of 12-HEPE as the dominant metabolite in skin after dietary intake of ω 3 fatty acid-rich linseed oil

To examine the metabolic progression of ω 3 fatty acids in the skin, mice were maintained with α -linolenic acid-rich linseed oil or control soybean oil for 2 months. LC-MS/MS analysis revealed that among the EPA-derived metabolites examined (ie, 5-, 12-, 15-, and 18-HEPE, 17,18-EpETE, and 17,18-diHETE), the concentrations of 12-HEPE and 15-HEPE were higher in the skin of linseed oil-fed mice than in the soybean oil-fed mice (Figure 1A). In addition, the concentration of 12-HEPE was higher than that of 15-HEPE, suggesting that 12-HEPE is the major EPA-derived metabolite in the skin. In the gut, the concentration of 17,18-EpETE was higher in the linseed oil-fed mice than in the soybean oil-fed mice, which is consistent with our previous data.³³ In order to demonstrate that metabolic progression of fatty acids are different among the tissues, the amount of 12-HEPE was compared between the skin and the gut. We found in the linseed oil-fed mice that the concentration of 12-HEPE was higher in the skin than in the gut (Figure S1A). Thus, these results suggest that the metabolic progression of dietary fatty acids is different between the skin and gut, and that 12-HEPE is the dominant EPA-derived metabolite in the skin.

We also examined the expression levels of four genes encoding enzymes involved in fatty acid metabolism (Figure 1B). The expression levels of *Alox12* and *Alox12b*, which encode 12-LOX enzymes that mediate hydroxylation of EPA for the generation of 12-HEPE,⁴⁵ were higher in the skin than in the gut. In contrast, the expression levels of *Cyp2c44* and *Cyp4f16*, which encode CYP enzymes that mediate epoxidation of EPA for the generation of 17,18-EpETE,^{46,47} were higher in the gut than in the skin. These results were consistent with our lipidomics analysis in the skin and the gut (Figure 1A).

We also investigated whether there were any strain differences between C57BL/6 and BALB/c mice and found that both strains showed similar gene expression profiles for *Alox12*, *Alox12b*, *Cyp2c44*, and *Cyp4f16* (Figure 1B and Figure S1B) and prominent production of 12-HEPE (Figure 1A and Figure S1C).

3.2 | 12-HEPE reduces inflammation of DNFB-induced CHS

We next examined whether 12-HEPE and 15-HEPE have any bioactivity in the regulation of immune system in the skin. DNFB-induced CHS mice were administered fatty acid metabolites by i.p. injection, and ear swelling was evaluated as a representative sign of inflammation (Figure S2). We found that i.p. injection of 12-HEPE decreased ear swelling compared with vehicle control, whereas injection of 15-HEPE did not. We previously reported that stereostructure is a critical determinant of the anti-inflammatory activity of 17,18-EpETE (ie, 17(*S*),18(*R*)- and 17(*R*),18(*S*)-EpETE),⁴⁸ which led us to examine whether 12(*S*)-HEPE and 12(*R*)-HEPE show different regulatory activities in CHS. We found that 12(*S*)-HEPE and 12(*R*)-HEPE both ameliorated ear swelling, indicating that the different isomers of 12-HEPE have similar anti-inflammatory activities.

Next, we evaluated how the route of administration of 12-HEPE affects its anti-inflammatory activity, because the route of administration can impact clinical usage. We found that topical application of 12-HEPE resulted in a greater reduction of inflammation compared with i.p. injection (Figure 2A). Histological examination of hematoxylin and eosin-stained ear skin sections revealed that 12-HEPE inhibited the development of epidermal edema and infiltration of inflammatory cells into the dermis (Figure 2B). In addition, topical application of 12-HEPE showed the amelioration of epidermal thickening. These results indicate that topical application of 12-HEPE exerts anti-inflammatory properties more efficiently than i.p. injection, suggesting that 12-HEPE preferentially acts on skin cells rather than circulating cells. In addition, we also measured the amount of 12-HEPE in the skin 30 min after i.p. injection or topical application and found that the amount of 12-HEPE in the skin was much higher after topical application than after i.p. injection (Figure S3), which is consistent with the observed differences in anti-inflammatory activity after topical application or i.p. injection.

We also examined the timing of topical application of 12-HEPE in our CHS model. Mice were treated with 12-HEPE at both the sensitization and elicitation phases (ie, on days 0 and 5) or at the elicitation phase only (ie, on day 5) (Figure 2C). We found that 12-HEPE inhibited the development of ear swelling irrespective of the timing of administration, suggesting that 12-HEPE exerts its anti-inflammatory activity

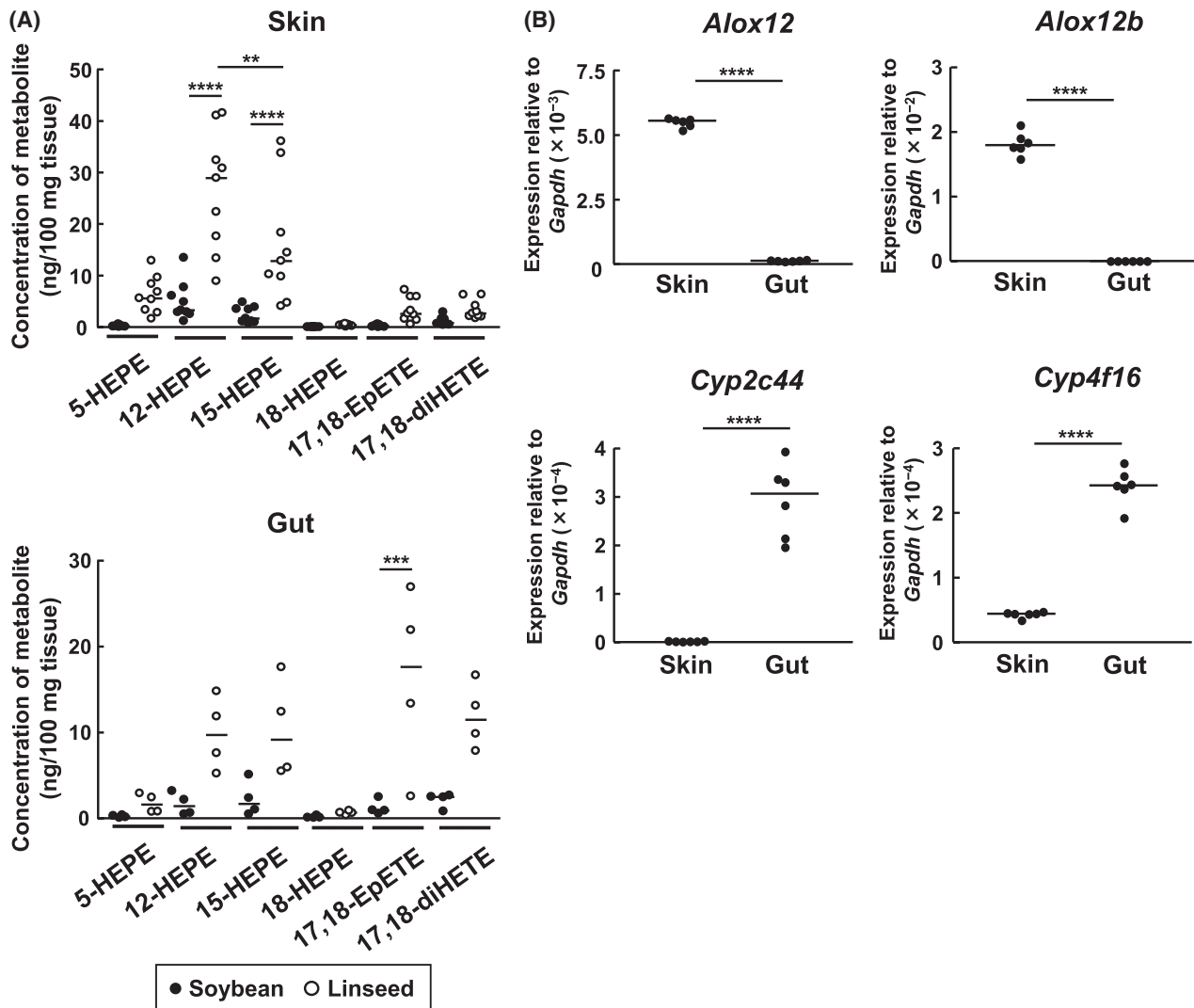


FIGURE 1 Identification of 12-hydroxyeicosapentaenoic acid (HEPE) as the dominant eicosapentaenoic acid (EPA)-derived metabolite, and 12-lipoxygenase as the main metabolic enzyme, in murine skin. A, BALB/c mice were maintained with feed containing ω 3 fatty acid-rich linseed oil or control soybean oil, and EPA-derived metabolites in the ear skin and gut were measured by liquid chromatography-tandem mass spectrometry. EpETE, epoxyeicosatetraenoic acid; diHETE, dihydroxyeicosatetraenoic acid. **, $P < .01$; ***, $P < .001$; ****, $P < .0001$ (Kruskal-Wallis test followed by Dunn's multiple comparison test). B, mRNA was isolated from the ear skin and gut of BALB/c mice, and quantitative real-time PCR analyses were performed to measure the expression levels of *Alox12*, *Alox12b*, *Cyp2c44*, and *Cyp4f16*, which were normalized to that of *Gapdh*. ****, $P < .0001$ (Mann-Whitney U test). In all panels, each point represents data from an individual mouse, and horizontal bars indicate median values

during the elicitation phase of CHS rather than during the sensitization phase. In support of this finding, we also found that 12-HEPE did not prevent the migration of skin dendritic cells to the draining lymph nodes (Figure S4A,B).

3.3 | Neutrophil recruitment is regulated by 12-HEPE treatment

We next investigated the mechanism underlying the inhibition of CHS by 12-HEPE. Because we found that the anti-inflammatory effects of 12-HEPE were exerted after the sensitization phase, we concentrated on the effects during the

elicitation phase only. We found that 12-HEPE did not affect DNFB-induced changes in vascular permeability or iSALT formation (Figure S4C,D), suggesting that 12-HEPE had little effect on mast cell degranulation and macrophage activity as iSALT inducer cells. In addition, flow cytometric analysis revealed that 12-HEPE did not change the number of IFN- γ -producing CD8⁺ T cells in the inflamed skin of CHS mice (Figure S4E), suggesting that 12-HEPE had little effect on T cell and dendritic cell activity. Consistent with the results that T cell number was not changed by 12-HEPE, we found that the expression level of two genes encoding T cell chemoattractants, *Cxcl9* and *Cxcl10*, were unchanged by 12-HEPE treatment after DNFB challenge (Figure S4F). Together,

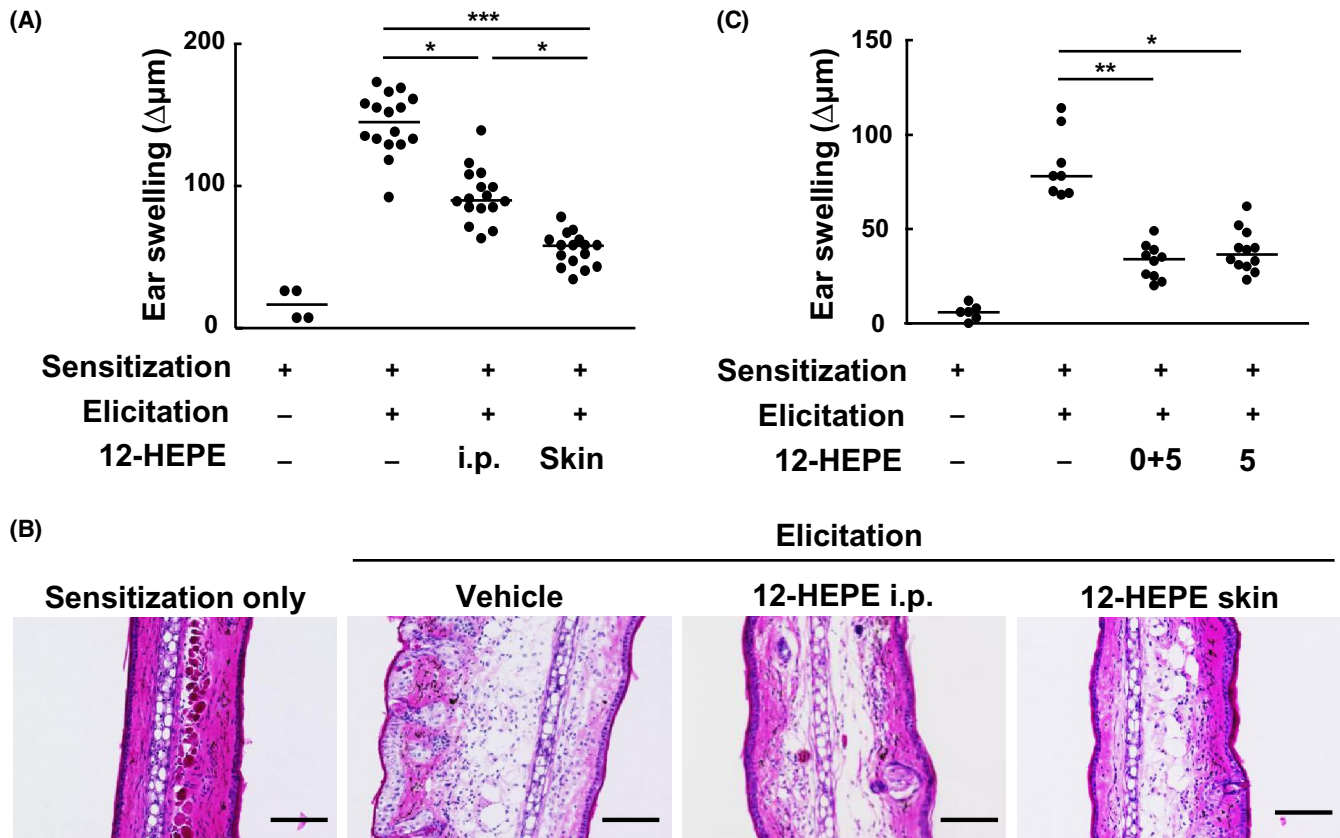


FIGURE 2 Topical application of 12-hydroxyeicosapentaenoic acid (HEPE) ameliorates inflammation more than intraperitoneal (i.p.) injection in mice with contact hypersensitivity. A, B, Mice were administered 12-HEPE (1 μg /administration) by i.p. injection or topical application (skin) or vehicle (50% [vol/vol] ethanol in PBS), by topical application on days 0 and 5 at 30 minutes before 2,4-dinitrofluorobenzene (DNFB) treatment. A, Ear swelling was evaluated on day 7. Data are combined from three independent experiments. B, Ear tissue samples were prepared on day 7, stained with hematoxylin and eosin, and analyzed histologically. Representative images from two independent experiments are shown. Bars, 100 μm . C, Mice were topically administered 12-HEPE (1 μg /administration) or vehicle (50% [vol/vol] ethanol in PBS) on days 0 and 5, or on day 5 only, at 30 minutes before DNFB treatment. On day 7, ear swelling was measured. Data are combined from two independent experiments. For panels A and C, each point represents data from an individual mouse, and horizontal bars indicate median values. *, $P < .05$; **, $P < .01$; ***, $P < .001$ (Kruskal-Wallis test followed by Dunn's multiple comparison test)

these findings suggest that 12-HEPE has no effect on mast cells, macrophages, dendritic cells, or T cells.

We next examined the impact of 12-HEPE on neutrophils as the inflammatory cells implicated in the development of CHS.^{16,19,20} Flow cytometric analyses revealed that topical application of 12-HEPE inhibited DNFB-induced neutrophil infiltration into the skin (Figure 3A,B). Immunohistological analysis also revealed that inflammation-associated infiltration of neutrophils into the dermis was inhibited by topical application of 12-HEPE (Figure 3C).

It has been reported that neutrophil infiltration is also inhibited by other EPA-derived metabolites, including resolvin E1 (RvE1), RvE2, and RvE3.^{43,49-51} These RvEs are produced from 18-HEPE, which led us to examine whether topical application of 18-HEPE also has anti-inflammatory effects in CHS. However, topical application of 18-HEPE had no effect on ear swelling or neutrophil infiltration into the skin (Figure S5A,B). This indicates that 12-HEPE plays a unique role in the regulation of CHS by inhibiting neutrophil migration.

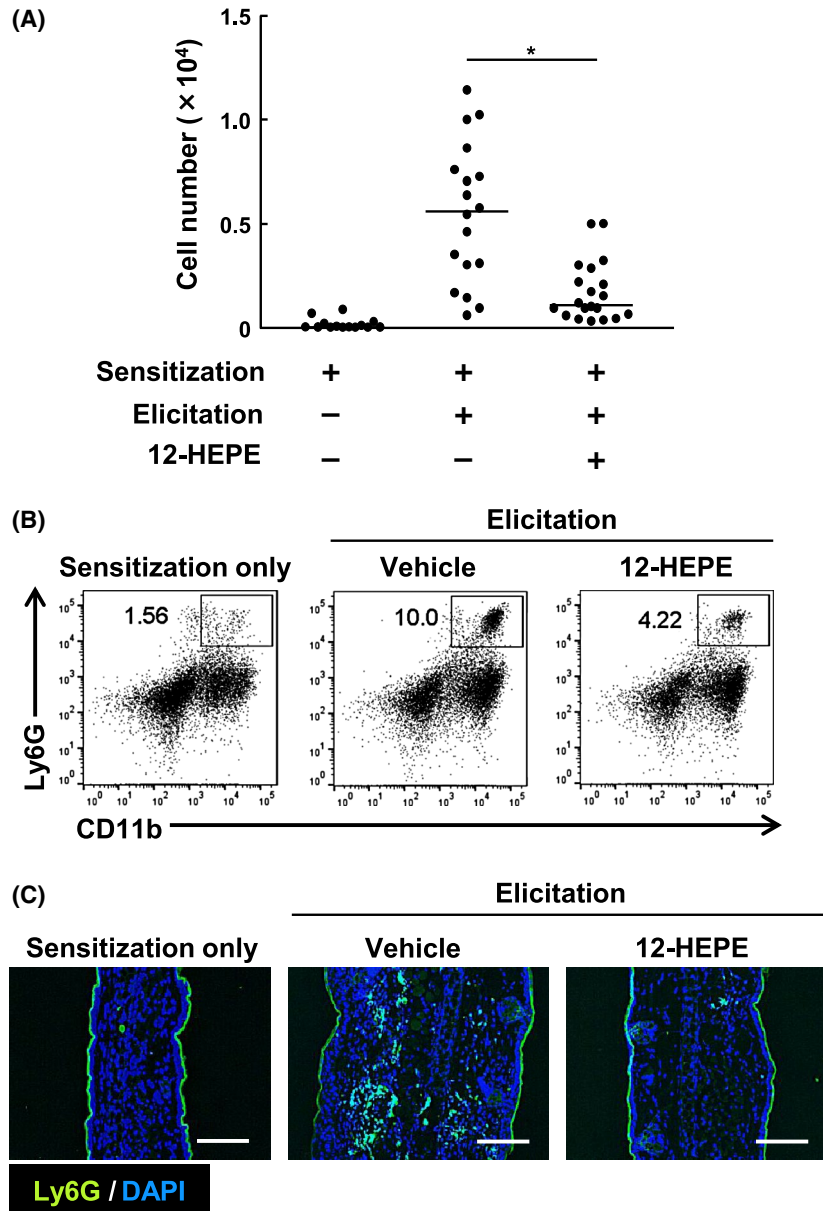
3.4 | Neutrophil recruitment is reduced by 12-HEPE via an indirect pathway

To elucidate whether 12-HEPE had a direct or indirect influence on neutrophil infiltration, we examined whether 12-HEPE inhibited neutrophil pseudopod formation, which is essential for neutrophil migration.^{52,53} We purified neutrophils from bone marrow; stimulated them with fMLP, a bacteria-derived neutrophil chemoattractant; and examined pseudopod formation by evaluating neutrophil actin polymerization. We found that fMLP-induced actin polymerization was not affected by 12-HEPE treatment (Figure S6), suggesting that 12-HEPE inhibits neutrophil infiltration through an indirect mechanism.

3.5 | 12-HEPE reduces CXCL1 and CXCL2 expression in human keratinocytes

The neutrophil chemoattractants CXCL1 and CXCL2, which are produced by keratinocytes, play important roles in the

FIGURE 3 12-Hydroxyeicosapentanoic acid (HEPE) reduces neutrophil recruitment to the inflamed skin of mice with contact hypersensitivity. A–C, Mice were topically administered 12-HEPE (1 $\mu\text{g}/\text{administration}$) or vehicle (50% [vol/vol] ethanol in PBS) on days 0 and 5 at 30 minutes before DNFB treatment. A, On day 7, the number of Ly6G⁺ CD11b⁺ neutrophils was determined on the basis of total cell numbers and flow cytometric data. Horizontal bars indicate median values. Data are combined from four independent experiments. *, $P < .05$ (Kruskal-Wallis test followed by Dunn's multiple comparison test). B, Representative flow cytometry profiles from four independent experiments showing neutrophils in ear samples on day 7. Neutrophils were gated as Ly6G⁺ CD11b⁺ cells. Numbers indicate the percentage of Ly6G⁺ CD11b⁺ neutrophils. C, Frozen ear sections obtained on day 7 were stained with fluorescein isothiocyanate-labeled Ly6G and 4',6-diamidino-2-phenylindole (DAPI) for immunohistologic analysis. Representative images from two independent experiments are shown. Bars, 100 μm



development of CHS,⁸⁻¹⁰ and their gene expression is induced by TNF- α produced by hapten-stimulated keratinocytes and mast cells.^{4,7,11} Therefore, we next examined the pathways through which regulation of these chemokines indirectly inhibits neutrophil infiltration. In mice, topical application of 12-HEPE reduced DNFB-induced expression levels of *Cxcl1* and *Cxcl2* at 6 hours after challenge compared with vehicle control (Figure 4A). We also confirmed that the gene expression level of *Tnf* was increased after elicitation by application of DNFB to the skin (Figure S7), but 12-HEPE did not affect the DNFB-induced induction of *Tnf* in inflamed ears (Figure S7), suggesting that 12-HEPE acts downstream of TNF- α .

Because keratinocytes are the most important source of chemokine production in response to TNF- α in the skin, we performed in vitro experiments using a human keratinocyte cell line, HaCaT cells.^{4,5} HaCaT cells were stimulated with TNF- α , and gene expression levels of the chemokines were analyzed

with quantitative real-time PCR. As previously reported,^{7,54} stimulation of HaCaT cells with TNF- α induced expression of *CXCL1* and *CXCL2*, but we also found that 12-HEPE inhibited the TNF- α -induced induction of these chemokines (Figure 4B).

3.6 | 12-HEPE exerts its anti-inflammatory actions via RXR α in keratinocytes

To identify the receptors associated with the anti-inflammatory activity of 12-HEPE, we evaluated the expression of genes encoding two G protein-coupled receptors (GPR40 and GPR120) and several nuclear receptors, including PPARs (PPAR α , β , and γ), RXRs (RXR α , β , and γ), and liver X receptors (LXR α and β), which are known as long-chain fatty acid receptors.⁵⁵⁻⁶⁰ Among these receptors, the expression level of *RXRA* and *Rxra* was highly observed in HaCaT cells and freshly isolated murine

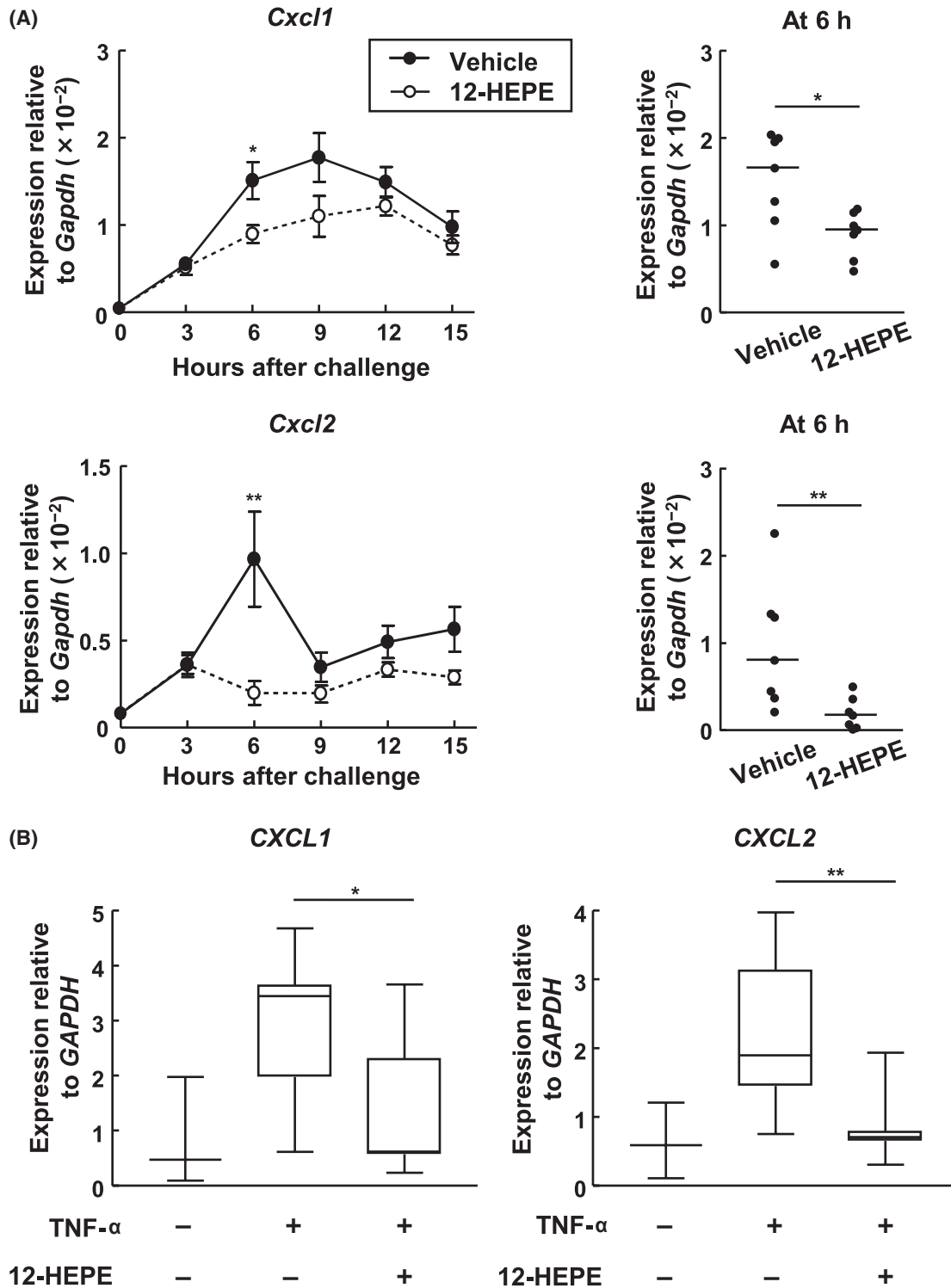


FIGURE 4 12-Hydroxyeicosapentaenoic acid (HEPE) downregulates *CXCL1* and *CXCL2* expression in keratinocytes. A, Mice were topically administered 12-HEPE (1 μ g/administration, open circles and dashed line) or vehicle (50% [vol/vol] ethanol in PBS, closed circles and solid line) on days 0 and 5 at 30 minutes before 2,4-dinitrofluorobenzene (DNFB) treatment. After DNFB treatment on day 5, ear skin, which was collected at the indicated time points, was homogenized for isolation of mRNA, and quantitative real-time PCR analysis was performed to measure the expression levels of *Cxcl1* and *Cxcl2*, which were normalized to that of *Gapdh*. Data are combined from two independent experiments (mean \pm SEM values; 0 hour, n = 8; 15 hours, n = 13; other groups, n = 7). Data at 6 hours after DNFB challenge are also shown as median values. Each point represents data from an individual mouse. *, $P < .05$; **, $P < .01$ (Mann-Whitney U test). B, HaCaT cells were treated with 12-HEPE (300 nmol/L) or vehicle (0.2% [vol/vol] ethanol in Dulbecco's modified Eagle's medium) for 30 minutes before stimulation with tumor necrosis factor (TNF)- α . The mRNA was isolated from HaCaT cells, and quantitative real-time PCR analysis was performed to measure the expression levels of *CXCL1* and *CXCL2*, which were normalized to the expression of *GAPDH*. The horizontal line in each box plot indicates the median value. Data are combined from three independent experiments (without TNF- α , n = 5; other groups, n = 10). *, $P < .05$; **, $P < .01$ (Kruskal-Wallis test followed by Dunn's multiple comparison test)

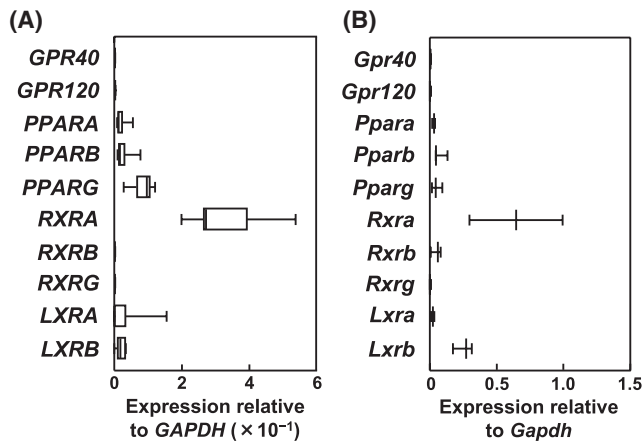


FIGURE 5 Retinoid X receptor (RXR) α is predominantly expressed in keratinocytes. A, mRNA was isolated from HaCaT cells, and quantitative real-time PCR analysis was performed to measure the expression levels of the indicated genes, which were normalized to that of *GAPDH*. B, CD45⁻ CD31⁻ CD34⁻ CD49f⁺ keratinocytes were sorted from ear skin of naïve mice, and quantitative real-time PCR analysis was performed to measure the expression levels of the indicated genes, which were normalized to that of *Gapdh*. The vertical line in each box plot indicates the median value (n = 4 or 8)

skin keratinocytes, respectively (Figure 5A,B), suggesting that RXR α is involved in the anti-inflammatory effect of 12-HEPE on keratinocytes. Then, we applied an RXR pan-antagonist (HX 531) to the CHS model, and found that it abolished the anti-inflammatory activities of 12-HEPE (Figure 6A-D).

Finally, we examined in more detail the involvement of RXR α in the inhibitory activity of 12-HEPE. We knocked down RXR α in HaCaT cells using a specific siRNA in vitro because the expression level of *RXRA* was much higher than that of the other RXR-encoding genes (ie, *RXRB* and *RXRG*) in keratinocytes (Figure 5). We first confirmed that RXR α -specific siRNA treatment efficiently reduced the amount of RXR α in HaCaT cells (Figure 7A), which coincidentally canceled the inhibitory effect of 12-HEPE on the expression of *CXCL1* and *CXCL2* induced by TNF- α (Figure 7B). We found that the expression of *Rxra* in bone marrow-derived neutrophils was much lower than that in keratinocytes (Figure S8), which is consistent with our findings that 12-HEPE did not have a direct effect on neutrophils (Figure S6). These findings suggest that RXR α is the receptor targeted by 12-HEPE for the inhibition of *CXCL1* and *CXCL2* production by keratinocytes.

4 | DISCUSSION

In this study, we identified 12-HEPE as the dominant metabolite in the skin of linseed oil-fed mice, and found that 12-HEPE exhibited anti-inflammatory activity for the amelioration of CHS by inhibiting the expression of two neutrophil chemoattractant-encoding genes, *CXCL1* and *CXCL2*, in keratinocytes in an RXR-dependent manner. Previously, we

found that dietary intake of linseed oil led to an increase in the level of the EPA-derived CYP metabolite 17,18-EpETE in the intestine and the EPA-derived 15-LOX metabolite 15-HEPE in the nasal passage, and that these two metabolites inhibited the development of food allergy and allergic rhinitis, respectively.^{33,37} We also identified the ω 3 docosapentaenoic acid-derived 12-LOX metabolite 14-hydroxydocosapentaenoic acid as being increased in the breast milk of linseed oil-fed mice, and that this metabolite inhibited the development of CHS in offspring.⁴² Together, our current and previous observations suggest that the metabolic progression of ω 3 fatty acids and the levels of metabolites produced differ among different tissues.

Regarding the roles of ω 3 fatty acid metabolites in the control of CHS, we previously reported that 17,18-EpETE attenuated skin inflammation in CHS to a greater extent when mice were treated with 17,18-EpETE via i.p. injection compared with via topical application, whereas our findings for 12-HEPE in the present study were the opposite.³⁸ This difference may reflect differences in the mechanisms of action of 17,18-EpETE and 12-HEPE. Indeed, 17,18-EpETE inhibited neutrophil migration by inhibiting pseudopod formation, whereas 12-HEPE did so by inhibiting the expression of *CXCL1* and *CXCL2* in keratinocytes. In addition to 17,18-EpETE and 12-HEPE, several other lipid mediators have been identified that inhibit CHS by targeting different cells. For example, oleic acid-derived mead acid acts directly on neutrophils to inhibit their migration and leukotriene B₄ production,⁴¹ and EPA-derived RvE1, which is a metabolite of 18-HEPE, impairs the mobility of cutaneous dendritic cells by blocking leukotriene B₄-leukotriene B₄ receptor 1 signaling, thereby reducing skin inflammation in CHS.³⁹ However, although 18-HEPE is a substrate of functional EPA-derived metabolites of RvEs, we found here that 18-HEPE had little effect on ear swelling, suggesting that 18-HEPE is not metabolized to RvEs. Indeed, conversion of 18-HEPE to RvE1 and RvE2 is mediated by 5-LOX, which is highly expressed in neutrophils, and to RvE3 is mediated by 12/15-LOX, which is highly expressed in eosinophils.^{43,51,61} Therefore, it is likely that 18-HEPE is not converted to RvEs in the absence of neutrophils in the early phase of inflammation. Compared with these other metabolites, 12-HEPE uniquely targets keratinocytes, in which it inhibits *CXCL1* and *CXCL2* gene expression. Because keratinocyte-derived *CXCL1* and *CXCL2* contribute to the development of several inflammatory skin diseases, including psoriasis and atopic dermatitis,^{5,6,62,63} 12-HEPE may be an effective molecule for the control of these skin diseases.

In the elicitation phase of CHS, the hapten triggers TNF- α production by keratinocytes, which activates nuclear factor- κ B (NF- κ B) signaling in keratinocytes in an autocrine manner, which leads to the production of *CXCL1*, *CXCL2*, *CXCL9*, and *CXCL10*.^{4,5} In murine skin, we found that 12-HEPE inhibited the induction of the expression of *Cxcl1*

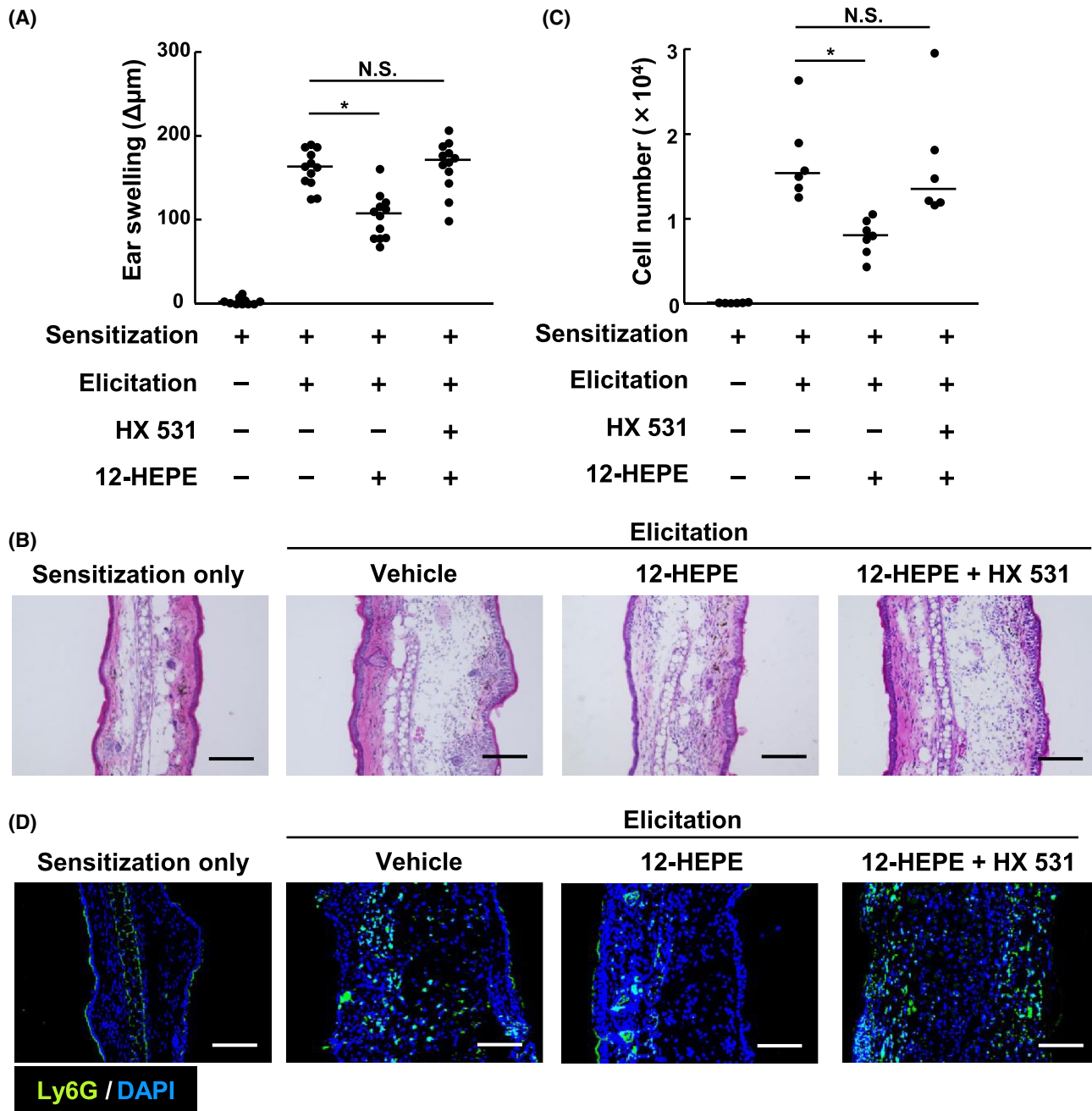


FIGURE 6 12-Hydroxyeicosapentaenoic acid (HEPE) ameliorates contact hypersensitivity via retinoid X receptor (RXR)-dependent mechanisms. A–D, Mice were topically administered 40 nmol of the RXR pan-antagonist HX 531 or vehicle (25% [vol/vol] dimethyl sulfoxide in PBS) on days 0 and 5. Sixty minutes later, 12-HEPE (1 $\mu\text{g}/\text{administration}$) or vehicle (50% [vol/vol] ethanol in PBS) were administered, followed 30 minutes later by treatment with 2,4-dinitrofluorobenzene. A, Ear swelling was evaluated on day 7. B, Samples of ear tissue were prepared on day 7, stained with hematoxylin and eosin, and analyzed histologically. Representative images from two independent experiments are shown. Bars, 100 μm . C, On day 7, the number of Ly6G⁺ CD11b⁺ neutrophils was determined on the basis of total cell numbers and flow cytometric data. Each point represents data from an individual mouse. Data are combined from two independent experiments. Horizontal bars indicate median values. *, $P < .05$; NS, not significant (Kruskal-Wallis test followed by Dunn's multiple comparison test). D, Frozen ear sections obtained on day 7 were stained with fluorescein isothiocyanate-labeled Ly6G and DAPI for immunohistologic analysis. Representative images from two independent experiments are shown. Bars, 100 μm

and *Cxcl2* but not of *Cxcl9* and *Cxcl10*. The TNF- α -NF- κ B-induced expression of *CXCL9* and *CXCL10* is enhanced by IFN- γ signaling,^{64,65} whereas IFN- γ has little effect on the expression of *CXCL1* and *CXCL2*.⁶⁶ In the present study,

12-HEPE did not block T cell infiltration, suggesting that T cell-derived IFN- γ stimulates keratinocytes to produce *CXCL9* and *CXCL10* for the recruitment of T cells to the skin.

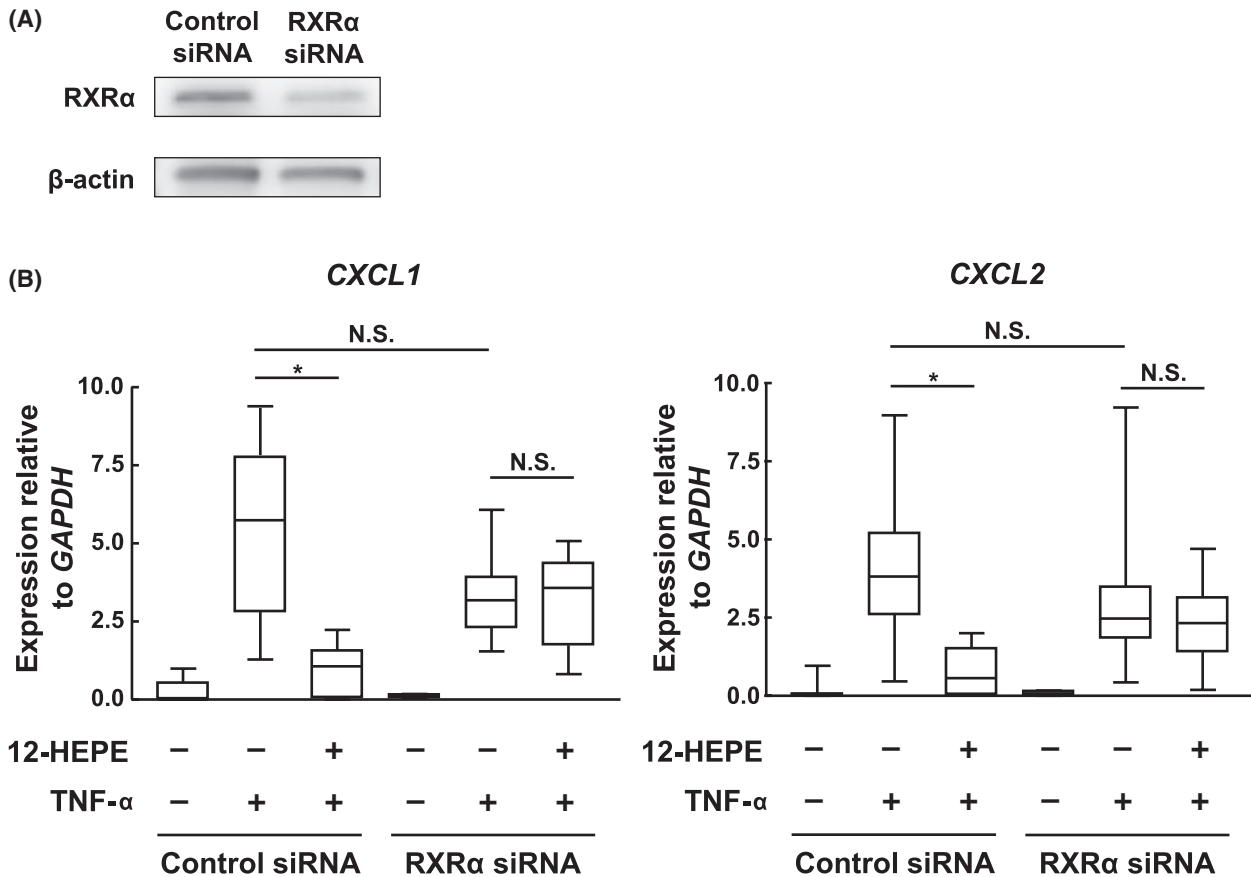


FIGURE 7 Essential role of retinoid X receptor (RXR) α on 12-hydroxyeicosapentaenoic acid (HEPE)-mediated chemokine suppression in keratinocytes. A, RXR α expression level in HaCaT cells treated with RXR α -specific siRNA or with nonspecific control siRNA as determined by western blotting using a specific anti-RXR α mAb. β -actin levels are shown as the control for equal protein loading. B, RXR α siRNA-transfected HaCaT cells or nonspecific control siRNA-transfected HaCaT cells were treated with 12-HEPE (300 nmol/L) or vehicle (0.2% [vol/vol] ethanol in Dulbecco's modified Eagle's medium) for 30 minutes before stimulation with tumor necrosis factor (TNF)- α . mRNA was isolated from the cells, and quantitative real-time PCR analysis was performed to measure the expression levels of *CXCL1* and *CXCL2*, which were normalized to the expression of *GAPDH*. Data are combined from three independent experiments (without TNF- α , n = 5; other groups, n = 10). The horizontal line in each box plot indicates the median value. *, $P < .05$; NS, not significant (Kruskal-Wallis test followed by Dunn's multiple comparison test)

In the present study, we also found that the anti-inflammatory activity of 12-HEPE was canceled in the presence of HX 531, a pan-antagonist of RXR. Although HX 531 targets three different RXR subtypes (ie, RXR α , RXR β , and RXR γ), we found that *RXR α* remained dominantly expressed in keratinocytes. Indeed, RXR α is reported to play important roles in the maintenance of skin homeostasis, because keratinocyte-selective ablation of RXR α results in hyperproliferation, abnormal differentiation, and inflammatory reaction by keratinocytes.⁶⁷⁻⁷⁰ In contrast, animals lacking RXR β or RXR γ do not show these skin abnormalities.^{71,72} In the present study, RXR α -specific siRNA experiments revealed that RXR α plays an essential role in the anti-inflammatory activities of 12-HEPE in keratinocytes. Taken together, these findings suggest that the 12-HEPE-RXR α axis, not axes involving RXR β and RXR γ , plays an important role in the maintenance of keratinocyte-mediated skin homeostasis. RXRs form heterodimers with other nuclear receptor family members.⁶⁰ A previous study demonstrated that an RXR

agonist decreased TNF- α -induced chemokine release by inhibiting mitogen-activated protein kinase and NF- κ B activation though RXR/PPAR γ heterodimer activation.⁷³ Although we detected the expression of PPAR γ in HaCaT cells, treatment with a PPAR γ antagonist (GW9662) had little effect on the function of 12-HEPE (Figure S9), suggesting that RXR/PPAR γ is unlikely to be a major target for 12-HEPE. Activation of RXR heterodimers other than RXR/PPAR γ may also play an important role in the downregulation and production of inflammatory chemokines. For example, it has been reported that the RXR/PPAR α axis inhibits NF- κ B transcription activity, and the RXR/PPAR β axis suppresses inflammatory interleukin-6 production.^{74,75} Agonist-activated RXR/PPAR complexes negatively regulate other transcription factors including NF- κ B and activator protein-1, which are involved in the promotion of *CXCL1* and *CXCL2* expression, thereby inhibiting its ability to induce gene transcription.^{66,75-78} For the remaining RXR heterodimer, RXR/LXR, an RXR agonist reduced translocation of NF- κ B into nuclei

by inducing activation transcription factor 3, which binds to the p65 component of NF- κ B.⁷⁹ These observations suggest that 12-HEPE may downregulate the expression of *CXCL1* and *CXCL2* by inhibiting NF- κ B and activator protein-1 via RXR α heterodimers with PPAR α , PPAR β , or LXRs.

In conclusion, we have shown that the metabolic progression of dietary ω 3 fatty acids differs in different organs, and we identified 12-HEPE as the dominant ω 3 fatty acid metabolite in skin. Furthermore, we found that 12-HEPE reduced the inflammation associated with CHS via RXR α -mediated inhibition of the expression of *CXCL1* and *CXCL2* in keratinocytes. Several stable analogs of fatty acid metabolites are currently undergoing drug development. For example, a stable analog of EPA-derived RvE1 has been shown to be effective for the treatment of dry-eye-associated inflammation.^{49,80} This RvE1 analog was also performed clinical trial for ocular inflammation and pain after cataract surgery.^{49,81} In addition, our previous work has demonstrated a correlation between infant allergic symptoms and a low concentration of an anti-inflammatory fatty acid metabolite of 14-hydroxydocosapentaenoic acid in breast milk.⁴² Therefore, fatty acid metabolites, including 12-HEPE, will be of interest as a novel target for drug development. Thus, our present findings provide valuable information for the development of 12-HEPE-based dietary and pharmaceutical strategies to ameliorate the skin inflammation associated with allergic contact dermatitis.

ACKNOWLEDGMENTS

This work was supported by the Ministry of Education, Culture, Sports, Science and Technology of Japan (MEXT)/Japan Society for the Promotion of Science KAKENHI (grant numbers JP19K07617 to TN; 19K08790 to TH; 15H05897 to MA; 18H02674 and 18H02150 to JK; and 15H05790 and 20H00534 to JK, TH, and KK); the Japan Agency for Medical Research and Development (AMED; JP20ek0410062s0202 to TH, JP19gm1210006 to KK, JP20ek0410062h0002 to JK and TH, and JP20ak0101068h0004 and JP20gm1010006h004 to JK); the Ministry of Health and Welfare of Japan and the Public/Private R&D Investment Strategic Expansion Program: PRISM (to JK); the Cross-ministerial Strategic Innovation Promotion Program: SIP (to JK); the Grant for Joint Research Project of the Institute of Medical Science, the University of Tokyo (to JK); the Ono Medical Research Foundation (to JK); and the Canon Foundation (to JK). The authors thank the laboratory members for their helpful discussions.

CONFLICT OF INTEREST

The authors have stated explicitly that there are no conflict of interest in connection with this article.

AUTHOR CONTRIBUTIONS

A. Saika, T. Nagatake, and J. Kunisawa conceived and designed the study, performed the data analysis, and wrote the manuscript.

A. Saika, T. Nagatake, S. Morimoto, E. Node, P. Tiwari, K. Hosomi, and A. Matsunaga performed the experiments and discussed the results. S.-I. Hirata, K. Sawane, J. Adachi, Y. Abe, J. Isoyama, T. Tomonaga, and M. Arita provided technical help for the LC-MS/MS analysis and discussed the results. T. Honda and K. Kabashima provided technical help for the skin inflammation animal model and discussed the results.

REFERENCES

- Kaplan DH, Igyártó BZ, Gaspari AA. Early immune events in the induction of allergic contact dermatitis. *Nat Rev Immunol.* 2012;12:114-124.
- Alinaghi F, Bennike NH, Egeberg A, Thyssen JP, Johansen JD. Prevalence of contact allergy in the general population: a systematic review and meta-analysis. *Contact Dermatitis.* 2019;80:77-85.
- Christensen AD, Haase C. Immunological mechanisms of contact hypersensitivity in mice. *APMIS.* 2012;120:1-27.
- Honda T, Egawa G, Grabbe S, Kabashima K. Update of immune events in the murine contact hypersensitivity model: toward the understanding of allergic contact dermatitis. *J Invest Dermatol.* 2013;133:303-315.
- Lee HY, Stieger M, Yawalkar N, Kakeda M. Cytokines and chemokines in irritant contact dermatitis. *Mediators Inflamm.* 2013;2013:916497.
- Sumida H, Yanagida K, Kita Y, et al. Interplay between CXCR2 and BLT1 facilitates neutrophil infiltration and resultant keratinocyte activation in a murine model of imiquimod-induced psoriasis. *J Immunol.* 2014;192:4361-4369.
- Griffin GK, Newton G, Tarrío ML, et al. IL-17 and TNF- α sustain neutrophil recruitment during inflammation through synergistic effects on endothelial activation. *J Immunol.* 2012;188:6287-6299.
- Dilulio NA, Engeman T, Armstrong D, Tannenbaum C, Hamilton TA, Fairchild RL. G α -mediated recruitment of neutrophils is required for elicitation of contact hypersensitivity. *Eur J Immunol.* 1999;29:3485-3495.
- Engeman T, Gorbachev AV, Kish DD, Fairchild RL. The intensity of neutrophil infiltration controls the number of antigen-primed CD8 T cells recruited into cutaneous antigen challenge sites. *J Leukoc Biol.* 2004;76:941-949.
- Cattani F, Gallese A, Mosca M, et al. The role of CXCR2 activity in the contact hypersensitivity response in mice. *Eur Cytokine Netw.* 2006;17:42-48.
- Dudeck A, Dudeck J, Scholten J, et al. Mast cells are key promoters of contact allergy that mediate the adjuvant effects of haptens. *Immunity.* 2011;34:973-984.
- Kish DD, Gorbachev AV, Parameswaran N, Gupta N, Fairchild RL. Neutrophil expression of Fas ligand and perforin directs effector CD8 T cell infiltration into antigen-challenged skin. *J Immunol.* 2012;189:2191-2202.
- Mantovani A, Cassatella MA, Costantini C, Jaillon S. Neutrophils in the activation and regulation of innate and adaptive immunity. *Nat Rev Immunol.* 2011;11:519-531.
- Jiang M, Fang H, Shao S, et al. Keratinocyte exosomes activate neutrophils and enhance skin inflammation in psoriasis. *FASEB J.* 2019;33:13241-13253.
- Oyoshi M, He R, Li Y, et al. Leukotriene B₄-driven neutrophil recruitment to the skin is essential for allergic skin inflammation. *Immunity.* 2012;37:747-758.

16. Weber FC, Németh T, Csepregi JZ, et al. Neutrophils are required for both the sensitization and elicitation phase of contact hypersensitivity. *J Exp Med*. 2015;212:15-22.
17. Chertov O, Yang D, Howard OM, Oppenheim JJ. Leukocyte granule proteins mobilize innate host defenses and adaptive immune responses. *Immunol Rev*. 2000;177:68-78.
18. Marzano AV, Ortega-Loayza AG, Heath M, Morse D, Genovese G, Cugno M. Mechanisms of inflammation in neutrophil-mediated skin diseases. *Front Immunol*. 2019;10:1059.
19. Christensen AD, Skov S, Haase C. The role of neutrophils and G-CSF in DNFB-induced contact hypersensitivity in mice. *Immun Inflamm Dis*. 2014;2:21-34.
20. Moniaga CS, Watanabe S, Honda T, Nielsen S, Hara-Chikuma M. Aquaporin-9-expressing neutrophils are required for the establishment of contact hypersensitivity. *Sci Rep*. 2015;5:15319.
21. Natsuaki Y, Egawa G, Nakamizo S, et al. Perivascular leukocyte clusters are essential for efficient activation of effector T cells in the skin. *Nat Immunol*. 2014;15:1064-1069.
22. Honda T, Kabashima K. Novel concept of iSALT (inducible skin-associated lymphoid tissue) in the elicitation of allergic contact dermatitis. *Proc Jpn Acad Ser B Phys Biol Sci*. 2016;92:20-28.
23. Akiba H, Kehren J, Ducluzeau MT, et al. Skin inflammation during contact hypersensitivity is mediated by early recruitment of CD8⁺ T cytotoxic 1 cells inducing keratinocyte apoptosis. *J Immunol*. 2002;168:3079-3087.
24. He D, Wu L, Kim HK, Li H, Elmets CA, Xu H. IL-17 and IFN-gamma mediate the elicitation of contact hypersensitivity responses by different mechanisms and both are required for optimal responses. *J Immunol*. 2009;183:1463-1470.
25. Vocanson M, Hennino A, Cluzel-Tailhardat M, et al. CD8⁺ T cells are effector cells of contact dermatitis to common skin allergens in mice. *J Invest Dermatol*. 2006;126:815-820.
26. Kish DD, Li X, Fairchild RL. CD8 T cells producing IL-17 and IFN-gamma initiate the innate immune response required for responses to antigen skin challenge. *J Immunol*. 2009;182:5949-5959.
27. Rauschenberger T, Schmitt V, Azeem M, et al. T cells control chemokine secretion by keratinocytes. *Front Immunol*. 2019;10:1917.
28. Calder PC. Session 3: joint nutrition society and irish nutrition and dietetic institute symposium on "nutrition and autoimmune disease" PUFA, inflammatory processes and rheumatoid arthritis. *Proc Nutr Soc*. 2008;67:409-418.
29. Calder PC. Very long-chain n-3 fatty acids and human health: fact, fiction and the future. *Proc Nutr Soc*. 2018;77:52-72.
30. Nagakura T, Matsuda S, Shichijyo K, Sugimoto H, Hata K. Dietary supplementation with fish oil rich in omega-3 polyunsaturated fatty acids in children with bronchial asthma. *Eur Respir J*. 2000;16:861-865.
31. Bargut TC, Ferreira TP, Daleprane JB, Martins MA, Silva PM, Aguila MB. Fish oil has beneficial effects on allergen-induced airway inflammation and hyperactivity in mice. *PLoS One*. 2013;8:e75059.
32. Hirakata T, Lee HC, Ohba M, et al. Dietary ω-3 fatty acids alter the lipid mediator profile and alleviate allergic conjunctivitis without modulating T. *FASEB J*. 2019;33:3392-3403.
33. Kunisawa J, Arita M, Hayasaka T, et al. Dietary ω3 fatty acid exerts anti-allergic effect through the conversion to 17,18-epoxyeicosatetraenoic acid in the gut. *Sci Rep*. 2015;5:9750.
34. Abdel Latif M, Abdul-Hamid M, Galaly SR. Effect of diethyl-carbamazine citrate and omega-3 fatty acids on trimellitic anhydride-induced rat skin allergy. *Asian Pac J Allergy Immunol*. 2015;33:33-41.
35. Dunstan JA, Mori TA, Barden A, et al. Fish oil supplementation in pregnancy modifies neonatal allergen-specific immune responses and clinical outcomes in infants at high risk of atopy: a randomized, controlled trial. *J Allergy Clin Immunol*. 2003;112:1178-1184.
36. Saika A, Nagatake T, Kunisawa J. Host- and microbe-dependent dietary lipid metabolism in the control of allergy, inflammation, and immunity. *Front Nutr*. 2019;6:36.
37. Sawane K, Nagatake T, Hosomi K, et al. Dietary omega-3 fatty acid dampens allergic rhinitis via eosinophilic production of the anti-allergic lipid mediator 15-hydroxyeicosapentaenoic acid in mice. *Nutrients*. 2019;11(12):2868.
38. Nagatake T, Shiogama Y, Inoue A, et al. The 17,18-epoxyeicosatetraenoic acid-G protein-coupled receptor 40 axis ameliorates contact hypersensitivity by inhibiting neutrophil mobility in mice and cynomolgus macaques. *J Allergy Clin Immunol*. 2018;142(2):470-484.e12. <https://doi.org/10.1016/j.jaci.2017.09.053>
39. Sawada YU, Honda T, Hanakawa S, et al. Resolvin E1 inhibits dendritic cell migration in the skin and attenuates contact hypersensitivity responses. *J Exp Med*. 2015;212:1921-1930.
40. Kulig P, Musiol S, Freiburger SN, et al. IL-12 protects from psoriasisiform skin inflammation. *Nat Commun*. 2016;7:13466.
41. Tiwari P, Nagatake T, Hirata SI, et al. Dietary coconut oil ameliorates skin contact hypersensitivity through mead acid production in mice. *Allergy*. 2019;74(8):1522-1532.
42. Hirata S-I, Nagatake T, Sawane K, et al. Maternal ω3 docosapentaenoic acid inhibits infant allergic dermatitis through TRAIL-expressing plasmacytoid dendritic cells in mice. *Allergy*. 2020;75(8):1939-1955.
43. Isobe Y, Arita M, Matsueda S, et al. Identification and structure determination of novel anti-inflammatory mediator resolvin E3, 17,18-dihydroxyeicosapentaenoic acid. *J Biol Chem*. 2012;287:10525-10534.
44. Boukamp P, Petrussevska RT, Breitkreutz D, Hornung J, Markham A, Fusenig NE. Normal keratinization in a spontaneously immortalized aneuploid human keratinocyte cell line. *J Cell Biol*. 1988;106:761-771.
45. Mashima R, Okuyama T. The role of lipoxygenases in pathophysiology; new insights and future perspectives. *Redox Biol*. 2015;6:297-310.
46. Isobe Y, Itagaki M, Ito Y, et al. Comprehensive analysis of the mouse cytochrome P450 family responsible for omega-3 epoxidation of eicosapentaenoic acid. *Sci Rep*. 2018;8:7954.
47. Wang WH, Zhang C, Lin DH, et al. Cyp2c44 epoxygenase in the collecting duct is essential for the high K⁺ intake-induced antihypertensive effect. *Am J Physiol Renal Physiol*. 2014;307:F453-F460.
48. Saika A, Nagatake T, Kishino S, et al. 17(S),18(R)-epoxyeicosatetraenoic acid generated by cytochrome P450 BM-3 from *Bacillus megaterium* inhibits the development of contact hypersensitivity via G-protein-coupled receptor 40-mediated neutrophil suppression. *FASEB BioAdvances*. 2020;2:59-71.
49. Serhan CN, Levy BD. Resolvins in inflammation: emergence of the pro-resolving superfamily of mediators. *J Clin Invest*. 2018;128:2657-2669.
50. Oh SF, Dona M, Fredman G, Krishnamoorthy S, Irimia D, Serhan CN. Resolvin E2 formation and impact in inflammation resolution. *J Immunol*. 2012;188:4527-4534.

51. Serhan CN, Clish CB, Brannon J, Colgan SP, Chiang N, Gronert K. Novel functional sets of lipid-derived mediators with antiinflammatory actions generated from omega-3 fatty acids via cyclooxygenase 2-nonsteroidal antiinflammatory drugs and transcellular processing. *J Exp Med*. 2000;192:1197-1204.
52. Weiner OD, Servant G, Welch MD, Mitchison TJ, Sedat JW, Bourne HR. Spatial control of actin polymerization during neutrophil chemotaxis. *Nat Cell Biol*. 1999;1:75-81.
53. Nishikimi A, Fukuhara H, Su W, et al. Sequential regulation of DOCK2 dynamics by two phospholipids during neutrophil chemotaxis. *Science*. 2009;324:384-387.
54. Guilloteau K, Paris I, Pedretti N, et al. Skin Inflammation Induced by the Synergistic Action of IL-17A, IL-22, Oncostatin M, IL-1alpha, and TNF-alpha Recapitulates Some Features of Psoriasis. *J Immunol*. 2010;184:5263-5270.
55. Wahli W, Michalik L. PPARs at the crossroads of lipid signaling and inflammation. *Trends Endocrinol Metab*. 2012;23:351-363.
56. Lengqvist J, Mata De Urquiza A, Bergman AC, et al. Polyunsaturated fatty acids including docosahexaenoic and arachidonic acid bind to the retinoid X receptor alpha ligand-binding domain. *Mol Cell Proteomics*. 2004;3:692-703.
57. Alvarez-Curto E, Milligan G. Metabolism meets immunity: the role of free fatty acid receptors in the immune system. *Biochem Pharmacol*. 2016;114:3-13.
58. Ecker J, Liebisch G, Patsch W, Schmitz G. The conjugated linoleic acid isomer trans-9, trans-11 is a dietary occurring agonist of liver X receptor alpha. *Biochem Biophys Res Commun*. 2009;388:660-666.
59. Bedi S, Hines GV, Lozada-Fernandez VV, et al. Fatty acid binding profile of the liver X receptor α . *J Lipid Res*. 2017;58:393-402.
60. Dawson MI, Xia Z. The retinoid X receptors and their ligands. *Biochim Biophys Acta*. 2012;1821:21-56.
61. Tjonahen E, Oh SF, Siegelman J, et al. Resolvin E2: identification and anti-inflammatory actions: pivotal role of human 5-lipoxygenase in resolvin E series biosynthesis. *Chem Biol*. 2006;13:1193-1202.
62. Lin ZC, Hsieh PW, Hwang TL, Chen CY, Sung CT, Fang JY. Topical application of anthranilate derivatives ameliorates psoriatic inflammation in a mouse model by inhibiting keratinocyte-derived chemokine expression and neutrophil infiltration. *FASEB J*. 2018;32(12):6783-6795. <https://doi.org/10.1096/fj.201800354>
63. Walsh CM, Hill RZ, Schwendinger-Schreck J, et al. Neutrophils promote CXCR3-dependent itch in the development of atopic dermatitis. *eLife*. 2019;8. <https://doi.org/10.7554/eLife.48448>
64. Kanda N, Shimizu T, Tada Y, Watanabe S. IL-18 enhances IFN-gamma-induced production of CXCL9, CXCL10, and CXCL11 in human keratinocytes. *Eur J Immunol*. 2007;37:338-350.
65. Ohmori Y, Schreiber RD, Hamilton TA. Synergy between interferon-gamma and tumor necrosis factor-alpha in transcriptional activation is mediated by cooperation between signal transducer and activator of transcription 1 and nuclear factor kappaB. *J Biol Chem*. 1997;272:14899-14907.
66. Burke SJ, Lu D, Sparer TE, et al. NF- κ B and STAT1 control CXCL1 and CXCL2 gene transcription. *Am J Physiol Endocrinol Metab*. 2014;306:E131-E149.
67. Li M, Indra AK, Warot X, et al. Skin abnormalities generated by temporally controlled RXRalpha mutations in mouse epidermis. *Nature*. 2000;407:633-636.
68. Li M, Chiba H, Warot X, et al. RXR-alpha ablation in skin keratinocytes results in alopecia and epidermal alterations. *Development*. 2001;128:675-688.
69. Li M, Messaddeq N, Teletin M, Pasquali JL, Metzger D, Chambon P. Retinoid X receptor ablation in adult mouse keratinocytes generates an atopic dermatitis triggered by thymic stromal lymphopoietin. *Proc Natl Acad Sci U S A*. 2005;102:14795-14800.
70. Gericke J, Ittensohn J, Mihály J, et al. Regulation of retinoid-mediated signaling involved in skin homeostasis by RAR and RXR agonists/antagonists in mouse skin. *PLoS One*. 2013;8:e62643.
71. Kastner P, Mark M, Leid M, et al. Abnormal spermatogenesis in RXR beta mutant mice. *Genes Dev*. 1996;10:80-92.
72. Huang P, Chandra V, Rastinejad F. Retinoic acid actions through mammalian nuclear receptors. *Chem Rev*. 2014;114:233-254.
73. Sanz MJ, Albertos F, Otero E, Juez M, Morcillo EJ, Piqueras L. Retinoid X receptor agonists impair arterial mononuclear cell recruitment through peroxisome proliferator-activated receptor- γ activation. *J Immunol*. 2012;189:411-424.
74. Onuki M, Watanabe M, Ishihara N, et al. A partial agonist for retinoid X receptor mitigates experimental colitis. *Int Immunol*. 2019;31:251-262.
75. Pawlak M, Lefebvre P, Staels B. Molecular mechanism of PPAR α action and its impact on lipid metabolism, inflammation and fibrosis in non-alcoholic fatty liver disease. *J Hepatol*. 2015;62:720-733.
76. Coll T, Barroso E, Alvarez-Guardia D, et al. The role of peroxisome proliferator-activated receptor beta/delta on the inflammatory basis of metabolic disease. *PPAR Res*. 2010;2010.
77. Lo HM, Lai TH, Li CH, Wu WB. TNF- α induces CXCL1 chemokine expression and release in human vascular endothelial cells in vitro via two distinct signaling pathways. *Acta Pharmacol Sin*. 2014;35:339-350.
78. McArdle JJ, Prescott CA. Age-based construct validation using structural equation modeling. *Exp Aging Res*. 1992;18:87-115.
79. Wang W, Nakashima KI, Hirai T, Inoue M. Anti-inflammatory effects of naturally occurring retinoid X receptor agonists isolated from *Sophora tonkinensis* Gagnep. via retinoid X receptor/liver X receptor heterodimers. *J Nat Med*. 2019;73:419-430.
80. ClinicalTrials.gov Website. C.T. Development America, Inc. A study of RX-10045 in the treatment of dry eye disease. <https://clinicaltrials.gov/ct2/show/NCT01675570>. Accessed November 23, 2020.
81. ClinicalTrials.gov Website. A.T. Resolve SARL. Efficacy and safety of RX-10045 ophthalmic solution for ocular inflammation and pain in cataract surgery. <https://clinicaltrials.gov/ct2/show/NCT02329743>. Accessed November 23, 2020.

SUPPORTING INFORMATION

Additional Supporting Information may be found online in the Supporting Information section.

How to cite this article: Saika A, Nagatake T, Hirata S-I, et al. ω 3 fatty acid metabolite, 12-hydroxyeicosapentaenoic acid, alleviates contact hypersensitivity by downregulation of *CXCL1* and *CXCL2* gene expression in keratinocytes via retinoid X receptor α . *The FASEB Journal*. 2021;35:e21354. <https://doi.org/10.1096/fj.202001687R>